

See discussions, stats, and author profiles for this publication at: <https://www.researchgate.net/publication/43199959>

One-Pot Protocol for Au-Based Hybrid Magnetic Nanostructures via a Noble-Metal-Induced Reduction Process

ARTICLE *in* JOURNAL OF THE AMERICAN CHEMICAL SOCIETY · MAY 2010

Impact Factor: 12.11 · DOI: 10.1021/ja100845v · Source: PubMed

CITATIONS

148

READS

100

2 AUTHORS:



Dingsheng Wang

Tsinghua University

92 PUBLICATIONS 2,918 CITATIONS

SEE PROFILE



Yadong Li

Tsinghua University

354 PUBLICATIONS 24,171 CITATIONS

SEE PROFILE

One-Pot Protocol for Au-Based Hybrid Magnetic Nanostructures via a Noble-Metal-Induced Reduction Process

Dingsheng Wang and Yadong Li*

State Key Laboratory of New Ceramics and Fine Processing, Department of Chemistry, Tsinghua University, Beijing 100084, P. R. China

Received January 30, 2010; E-mail: ydli@mail.tsinghua.edu.cn

In the past decades, catalysts based on Au nanoparticles have attracted considerable attention.^{1,2} However, because of the limited reserves of Au materials, it is urgent to reduce their usage. As we know, complex nanoobjects containing two or more different materials in the same nanoparticle can not only combine properties of the individual constituents but also show unique and superior properties different from ordinary materials.^{3–10} Therefore, hybrid nanocrystals consisting of Au and non-noble metals (particularly inexpensive first-row transition metals) may offer opportunities for reducing Au usage and the overall cost of catalysts.^{11,12} Furthermore, when magnetic heterometals (e.g., Co, Ni) are incorporated into Au nanoparticles, we can obtain Au-based magnetic heterostructured nanocatalysts.^{13–15} Magnetic catalysts can be reclaimed via magnetic separation after use, which would be very significant in preventing waste of Au materials. At present, although various methods have been developed for the preparation of hybrid nanocrystals, including core–shell particles with controlled shapes,^{16–22} exploiting a new idea for their facile and general synthesis still remains great challenge.

Herein, we present a one-pot wet chemical route to the synthesis of Au-based hybrid magnetic nanostructures, including Au–Co core–shell nanocrystals and Au–Ni spindly nanostructures. In a typical synthesis of Au–Co core–shell nanocrystals, HAuCl₄ and Co(NO₃)₂·6H₂O were used as the starting materials, and octadecylamine (ODA) was applied as both the solvent and the surfactant. The reaction was performed in air and finished within 10 min (for the detailed procedure, see the Supporting Information). Figure 1a shows a transmission electron microscopy (TEM) image of an as-obtained sample. The darker cores and the lighter shells in the TEM image suggest the formation of core–shell structures with a core diameter of ~10 nm and a shell thickness of ~5 nm. A powder X-ray diffraction (XRD) experiment was carried out to determine the crystal structure of the products. Two series of Bragg reflections were found, corresponding to cubic-phase Au (JCPDS 65-8601) and cubic-phase Co (JCPDS 15-0806) (Figure S1 in the Supporting Information). To further confirm the composition of the samples, energy-dispersive spectroscopy (EDS) was performed on an individual nanocrystal. The spectrum in Figure S2 shows only Au and Co peaks in addition to the two Cu peaks generated by the copper grid. Figure 1b shows a high-resolution TEM (HRTEM) image of a single crystal. The measured lattice spacings of 0.235 nm for the core and 0.205 nm for the shell correspond to cubic Au(111) and cubic Co(111) planes, respectively, indicating the formation of Au core–Co shell nanostructures. From the high-angle annular dark-field scanning TEM (HAADF-STEM) image depicted in Figure 1c, it is clear that core–shell structure was obtained (the brighter contrast in the image indicates the heavier element, Au). EDS mapping of a single particle indicates that Co encircles Au (Figure 1c inset and Figure S3). The line scanning analysis data show different distributions of Au and Co (Figure S4). These results confirm the as-synthesized Au core–Co shell hybrid nanostructures.

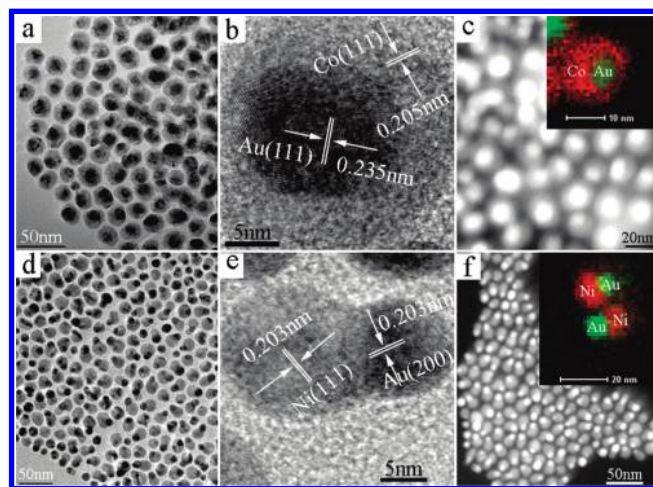


Figure 1. (a) TEM, (b) HRTEM, and (c) HAADF-STEM images of Au–Co core–shell nanocrystals and (d) TEM, (e) HRTEM, and (f) HAADF-STEM images of Au–Ni spindly nanostructures.

To further confirm this Au–Co core–shell structure, we treated the samples with nitric acid (nitric acid can dissolve Co but not Au). After the reaction, the products were collected and characterized using XRD and TEM. The XRD pattern (Figure S5) proved the formation of pure Au, and the TEM image (Figure S6) revealed them to be solid particles with average diameter of 10 nm. Hollow-structured particles were not obtained after treatment, indicating that the core is Au and the shell is Co.

This facile protocol also applies to synthesis of other Au-based hybrid nanostructures. For example, with a similar procedure, Au–Ni hybrid nanocrystals were also successfully prepared simply by replacing Co(NO₃)₂·6H₂O with Ni(NO₃)₂·6H₂O. Figure S7 shows the XRD pattern of as-obtained products, from which it can be observed that cubic-phase Au (JCPDS 65-8601) and cubic-phase Ni (JCPDS 65-2865) were formed in our synthesis. The TEM image (Figure 1d) displays the spindle-like morphology of the Au–Ni hybrid nanocrystals. The tip size is ~10 nm, and the tail diameter is ~15 nm. The EDS spectrum (Figure S8) confirms that the samples contain only Au and Ni. The HRTEM image of a single particle (Figure 1e) reveals clear lattice fringes with interplanar distances of 0.203 nm in both the tip and the tail. These spacings are characteristic of cubic Au in the (200) plane and cubic Ni in the (111) plane, respectively. The HAADF-STEM image shown in Figure 1f clearly displays the as-synthesized hybrid nanostructures. The EDS mapping results (Figure 1f inset and Figure S9) and line elemental EDS data (Figure S10) across a pair of particles further confirm that the tip is Au and the tail is Ni.

In ODA solvent, transition metal ions (Co²⁺, Ni²⁺) cannot be reduced (eqs 1 and 2):²³



However, noble and non-noble metal ions can be coreduced by ODA (eq 3):



This chemical process, namely, reduction of non-noble metal ions induced by a noble metal in the ODA system, is interesting and exciting. Figure 2 illustrates the noble-metal-induced reduction (NMIR) process. In the ODA system, Au^{3+} can obtain electrons from ODA and be reduced to Au (step I).²⁴ As soon as the Au forms, it is surrounded by an electron cloud offered by free electrons of other Au atoms. M^{2+} ($\text{M} = \text{Co}, \text{Ni}$) cannot be directly reduced by either ODA or Au, but it can be adsorbed on the surface of Au and share a small portion of the electron cloud through its empty orbital (step II). This causes the spherical electron cloud distribution surrounding Au to become an elliptical distribution. The shift in the electron cloud leads to partial positive charge on the Au surface, which is immediately neutralized by electrons offered by ODA. The continual supply of electrons from ODA to Au makes the shift in the electron cloud from Au to M occur continuously until M^{2+} is reduced completely.

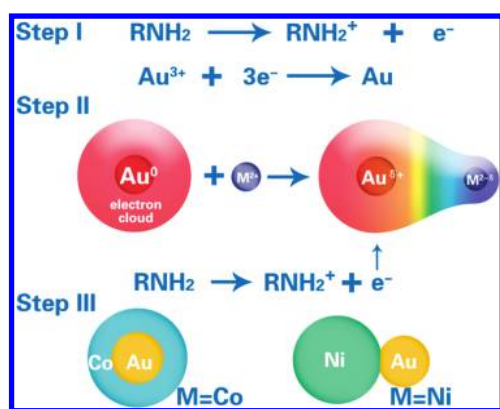


Figure 2. Schematic illustration of the NMIR synthetic strategy.

Although reduction of transition-metal ions by ODA or noble metals is thermodynamically unviable, the coexistence of ODA and noble metals makes the reduction of transition-metal ions viable. We believe that noble metals reduced by ODA play a key role in transferring electrons from ODA to the transition-metal ions. After the noble and non-noble metals are reduced, the kinetic parameters determine whether they form core-shell, spindle, or other structures (step III). Therefore, the NMIR strategy not only achieves a one-pot synthesis of multi-component nanocrystals but also shows an abnormal and novel chemical process. Our ongoing work has shown that various bimetallic nanocrystals consisting of noble (Pt, Pd, Rh, Ru, etc.) and non-noble (Fe, Co, Ni, Cu, Zn, etc.) metals can also be prepared via this strategy. More importantly, this NMIR strategy indicates that bimetallic nanocrystals might be successfully obtained in any synthetic system that applies to the preparation of noble-metal nanocrystals.

The Au-Co and Au-Ni hybrid nanocrystals synthesized using our system show strong magnetism (Figure S11). Figure S12 shows temperature-dependent zero-field-cooling (ZFC) and field-cooling (FC) measurement results for Au-Co and Au-Ni nanocrystals. These

results indicate that the nanocrystals can be reclaimed via magnetic separation after they are used as catalysts. In order to illuminate their superior catalytic properties, we used Au-Co core-shell nanocrystals as an example to investigate the catalytic activity toward CO oxidation. Figure S13 presents the CO percentage conversion as a function of reaction temperature for Au@Co nanocatalysts. For comparison, the catalytic activities of pure Au and Co for CO oxidation were also tested. The results indicate that the Au@Co particles indeed show better catalytic efficiency than pure Au or Co particles. Therefore, incorporating magnetic heterometals into Au nanoparticles not only can endow them with strong magnetism, which would be very essential in reclaiming the noble metals, but also can retain the desirable catalytic properties, which would be an indication of the possibility of partially replacing noble-metal catalysts with non-noble metals.

In conclusion, an effective NMIR synthetic strategy for synthesizing Au-Co core-shell nanocrystals and Au-Ni spindle nanostructures has been designed. This NMIR process provides new insights into the reduction of metal ions in organic solvents. It is believed that this novel strategy can be used to easily achieve the synthesis of various bimetallic nanocrystals, which would be of great significance in investigating their unique properties.

Acknowledgment. This work was supported by the NSFC (20921001, 90606006) and the State Key Project of Fundamental Research for Nanoscience and Nanotechnology (2006CB932300). We thank Weimeng Chen and Prof. Chinping Chen for characterizing the magnetic properties of the products.

Supporting Information Available: Experimental procedures, detailed characterization of products, and Figures S1–S13. This material is available free of charge via the Internet at <http://pubs.acs.org>.

References

- (1) Gorin, D. J.; Sherry, B. D.; Toste, F. D. *Chem. Rev.* **2008**, *108*, 3351.
- (2) Wang, D. S.; Xie, T.; Li, Y. D. *Nano Res.* **2009**, *2*, 30.
- (3) Gu, H.; Yang, Z.; Guo, J.; Chang, C. K.; Xu, B. *J. Am. Chem. Soc.* **2005**, *127*, 34.
- (4) Cable, R. E.; Schaak, R. E. *J. Am. Chem. Soc.* **2006**, *128*, 9588.
- (5) Wang, L. L.; Johnson, D. D. *J. Am. Chem. Soc.* **2009**, *131*, 14023.
- (6) Shevchenko, E. V.; Bodnarchik, M. I.; Kovalenko, M. V.; Talapin, D. V.; Smith, R. K.; Aloni, S.; Heiss, W.; Alivisatos, A. P. *Adv. Mater.* **2008**, *20*, 4323.
- (7) Yu, H.; Chen, M.; Rice, P. M.; Wang, S. X.; White, R. L.; Sun, S. H. *Nano Lett.* **2005**, *5*, 379.
- (8) Xu, C. J.; Wang, B. D.; Sun, S. H. *J. Am. Chem. Soc.* **2009**, *131*, 4216.
- (9) Buonsanti, R.; Grillo, V.; Carlino, E.; Giannini, C.; Gozzio, F.; Garcia-Hernandez, M.; Garcia, M. A.; Cingolani, R.; Cozzoli, P. D. *J. Am. Chem. Soc.* **2010**, *132*, 2437.
- (10) Lee, Y. M.; Garcia, M. A.; Huls, N. A. F.; Sun, S. H. *Angew. Chem., Int. Ed.* **2010**, *49*, 1271.
- (11) Bao, Y.; Calderon, H.; Krishnan, K. M. *J. Phys. Chem. C* **2007**, *111*, 1941.
- (12) Chen, D.; Li, J.; Shi, C.; Du, X.; Zhao, N.; Sheng, J.; Liu, S. *Chem. Mater.* **2007**, *19*, 3399.
- (13) Mandal, S.; Krishnan, K. M. *J. Mater. Chem.* **2007**, *17*, 372.
- (14) Bao, F.; Li, J. F.; Ren, B.; Yao, J. L.; Gu, R. A.; Tian, Z. Q. *J. Phys. Chem. C* **2008**, *112*, 345.
- (15) Wei, W.; Li, S.; Millstone, J. E.; Banholzer, M. J.; Chen, X.; Xu, X.; Schatz, G. C.; Mirkin, C. A. *Angew. Chem., Int. Ed.* **2009**, *48*, 4210.
- (16) Choi, S. H.; Na, H. B.; Park, Y. I.; An, K.; Kwon, S. G.; Jang, Y.; Park, M.-h.; Moon, J.; Son, J. S.; Song, I. C.; Moon, W. K.; Hyeon, T. *J. Am. Chem. Soc.* **2008**, *130*, 15573.
- (17) Lu, Y.; Zhao, Y.; Yu, L.; Dong, L.; Shi, C.; Hu, M.-J.; Xu, Y.-J.; Wen, L.-P.; Yu, S.-H. *Adv. Mater.* **2010**, *22*, 1407.
- (18) Shi, W. L.; Zeng, H.; Sahoo, Y.; Ohulchanskyy, T. Y.; Ding, Y.; Wang, Z. L.; Swihart, M.; Prasad, P. N. *Nano Lett.* **2006**, *6*, 875.
- (19) Yin, Y. D.; Rioux, R. M.; Erdonmez, C. K.; Hughes, S.; Somorjai, G. A.; Alivisatos, A. P. *Science* **2004**, *304*, 711.
- (20) Gao, J. H.; Zhang, B.; Gao, Y.; Pan, Y.; Zhang, X. X.; Xu, B. *J. Am. Chem. Soc.* **2007**, *129*, 11928.
- (21) Xie, R. G.; Peng, X. G. *Angew. Chem., Int. Ed.* **2008**, *47*, 7677.
- (22) Dong, H. C.; Zhu, M. Z.; Yoon, J. A.; Gao, H. F.; Jin, R. C.; Matyjaszewski, K. *J. Am. Chem. Soc.* **2008**, *130*, 12852.
- (23) Wang, D. S.; Xie, T.; Peng, Q.; Zhang, S. Y.; Chen, J.; Li, Y. D. *Chem.-Eur. J.* **2008**, *14*, 2507.
- (24) Zheng, H.; Smith, R. K.; Jun, Y.; Kisielowski, C.; Dahmen, U.; Alivisatos, A. P. *Science* **2009**, *324*, 1309.

JA100845V